thermo scientific

Cryo-electron microscopy applications

Cryo-electron microscopy (Cryo-EM) allows the structural analysis of protein complexes flash-frozen in their near-native states. You can now directly visualize not just large macromolecules but also smaller proteins complexes, including membrane proteins. This powerful technique can be used to complement traditional methods, such as X-ray crystallography (XRD) or nuclear magnetic resonance (NMR) for structure-based drug discovery.

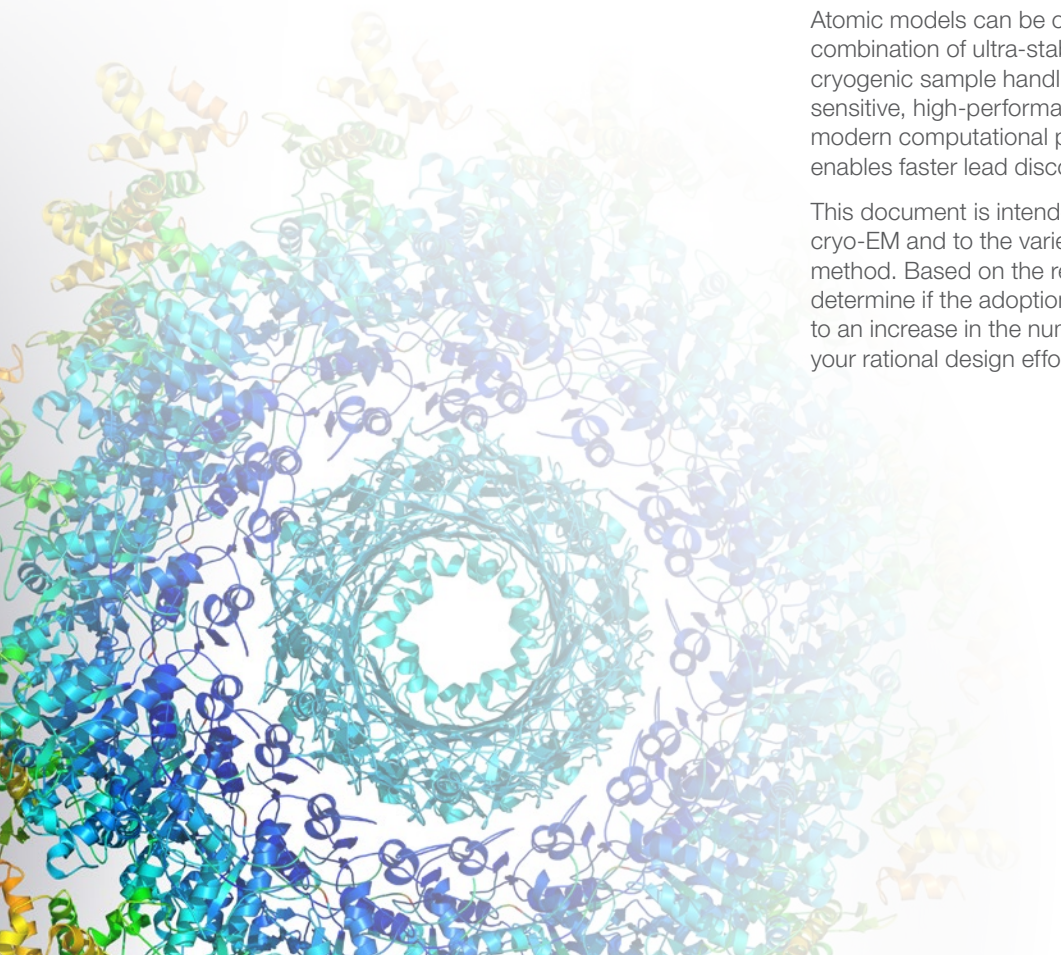

Cryo-EM enables structural analysis of protein complexes, providing better insight into all classes of biomolecules, including proteins that are difficult to work with. This method reveals detailed structural features of targets, ligands and their interactions at the atomic level, reducing the development time and guesswork of lead compound design.

Additionally, by capturing a series of intermediate states from a reaction mixture, “time-resolved” EM is possible, providing structural information over the course of a reaction. Conformational analysis of these intermediates provides unique, physiologically relevant details of disease mechanisms.

Even intractable targets are laid bare by cryo-EM. You can now analyze sample amounts that are generally too small for other techniques. No crystallization, concentrated solutions or epitope labeling are needed, meaning ion channels, transporters and receptors can now be analyzed. Additionally, membrane protein complexes in their native lipid environment can now be observed, thanks to lipid nanodiscs combined with cryo-EM single particle analysis (SPA).

Atomic models can be obtained with cryo-EM due to the combination of ultra-stable microscopes with automatic cryogenic sample handling, cameras that are fast and super sensitive, high-performance image processing procedures, and modern computational power. The acquisition of such models enables faster lead discovery and better lead optimization.

This document is intended to introduce you to the versatility of cryo-EM and to the variety of benefits made possible with this method. Based on the results of these applications, you can determine if the adoption of cryo-EM for your projects can lead to an increase in the number of valid results, thereby improving your rational design efforts.

ThermoFisher SCIENTIFIC

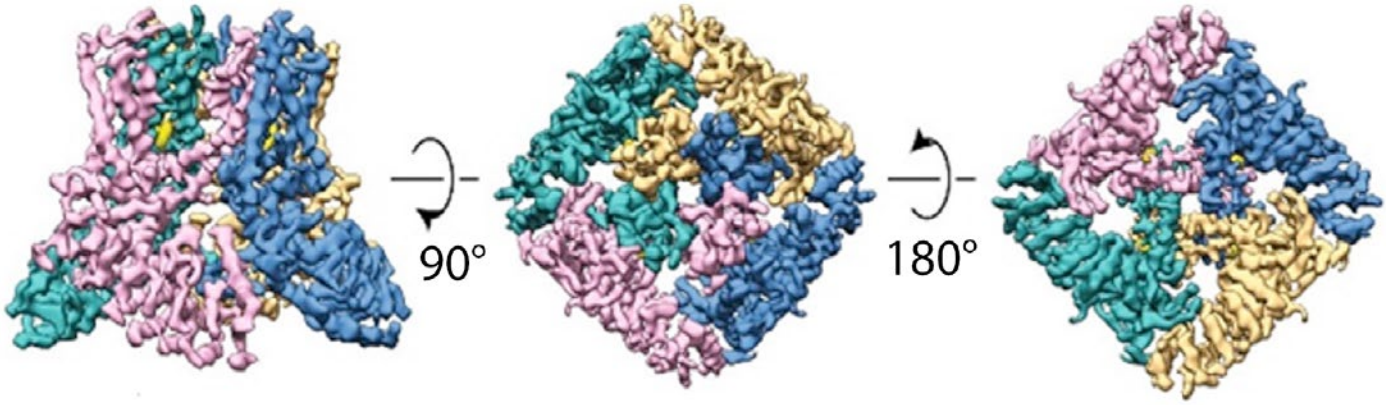

TRPV5 (Transient receptor potential cation channel subfamily V member 5) bound to an econazole inhibitor. Adapted from TET Hughes et al, Structural basis of TRPV5 channel inhibition by econazole revealed by cryo-EM.

Ion channels

"The requirement of X-ray crystallography is that you need to obtain a diffracting crystal to get atomic resolution. That has been a big hurdle if you're working on challenging targets. Almost every target we're working on now is very challenging."

- Dr. Seungil Han, Associate Research Fellow, Pfizer, Groton, CT

Ion channels, as the primary means of transport and exchange between cells, are a key subject of research. They critically impact the function of many diseases; however, they are challenging therapeutic targets because they are very difficult to crystallize. Once extracted from their native membrane environment, ion channels' structures collapse.

Additionally, cryo-EM can reveal not only the structure of an ion channel in its native lipid environment but also the various discreet open and closed states, which are critical to understanding ion gating mechanisms.

"Cryo-EM is undoubtedly the technique of choice to use for determining multiple conformation states of ion channels."

- Carus Lau et al. J Physiol 596.7 (2018) pp 1107–1119.

Insulin binding

Medical advances have made diabetes a manageable disease, providing its sufferers with longer, healthier lives. However, until recently, the binding mode of insulin to its receptor was unknown. Knowing the precise mechanism of binding could lead to the development of more effective therapeutics.

"The insulin receptor (IR) is a dimeric protein that plays a crucial role in controlling glucose homeostasis, regulating lipid, protein and carbohydrate metabolism, and modulating brain neurotransmitter levels. IR dysfunction has been associated with many diseases, including diabetes, cancer, and Alzheimer's disease."

- Dr. Giovanna Scapin, Senior Principal Scientist, Merck & Co.

Dr. Giovanna Scapin, Principal Scientist at Merck, has spent years studying insulin and diabetes. She was also one of the first adopters of cryo-EM. Thanks to single particle analysis, her team was able to ascertain the precise interaction between insulin and the insulin receptor, opening up exciting new avenues in drug discovery.

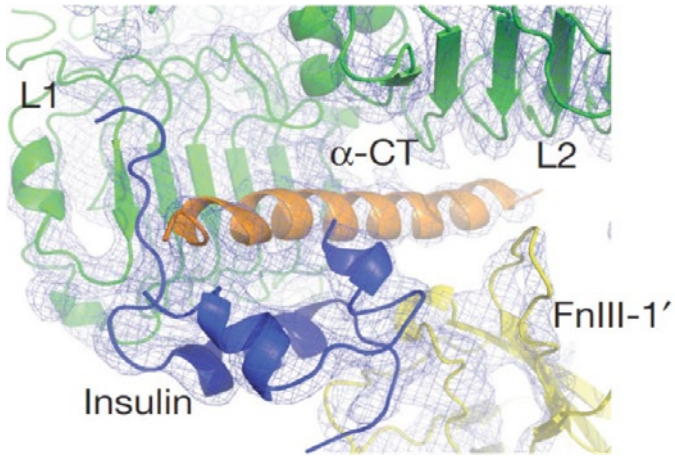

Electron density map obtained from cryo-EM (wireframe). The corresponding receptor-insulin complex structure is overlaid. Figure adapted from G. Scapin, et al. Structure of the insulin receptor-insulin complex by single particle cryoEM analysis. Nature 556, p. 122–125 April 5, 2018.

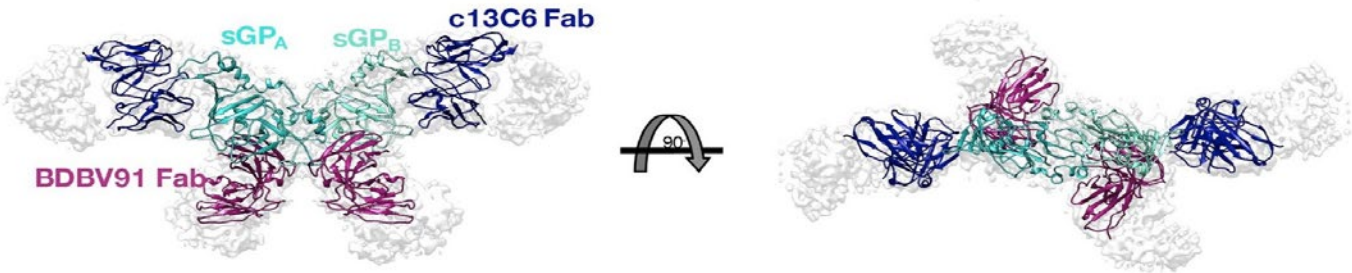

Electron density map of fragment antigen binding to sGP, obtained with single particle analysis. Figure adapted from J. Pallesen et al, Structures of Ebola virus GP and sGP in complex with therapeutic antibodies. Nature Microbiology v. 1, article number: 16128, 2016.

Viruses and antibodies

The Ebola virus causes severe hemorrhagic fever in humans and non-human primates. Currently, no approved therapeutic countermeasures exist. The virulence of Ebola may be partially attributed to the secreted glycoprotein (sGP), which is the main product transcribed from its GP gene. sGP is secreted from infected cells and can be readily detected in the serum of Ebola-infected hosts. Understanding the binding mechanism between this protein and its antibody could inform the future design of vaccines and treatments.

Dr. Andrew Ward's group at the Scripps Research Institute used 4.3 Å resolution cryo-EM to inform antibody epitope mapping, providing a basis to evaluate patients and vaccine antibody responses.

GPCR function

G protein-coupled receptors (GPCRs) are membrane proteins that regulate a variety of cellular responses to external stimuli. They are involved in a wide range of diseases and are a critical drug target; more than 50% of modern protein-based pharma is related to GPCRs. As membrane proteins, they are large, flexible and resistant to crystallization, meaning traditional analytical techniques such as NMR and XRD cannot be used to characterize their structures.

A collaborative project performed in conjunction with Dr. Mazdak Radjainia, a staff scientist at Thermo Fisher Scientific, successfully employed cryo-EM to analyze the GPCR structure. In addition, researchers were able to capture the dynamic nature of these complexes, as structural families can be grouped and individually characterized using cryo-EM.

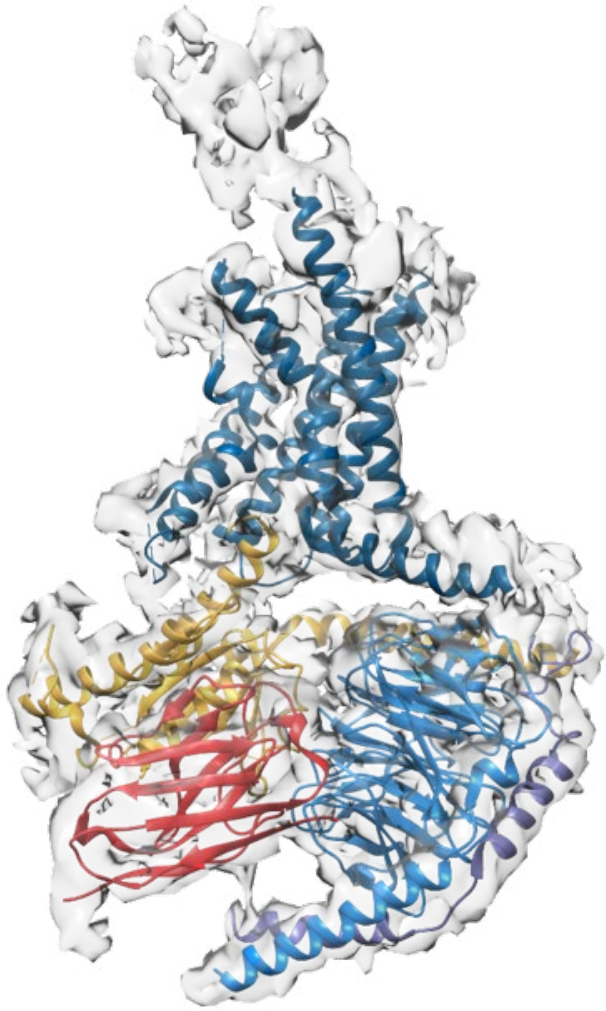

Cryo-EM density map of a GPCR complex. Figure created in Chimera (PDB ID: 5UZ7), adapted from Liang, YL et al. Phase-plate cryo-EM structure of a class B GPCR–G-protein complex. Nature v. 546, p. 118–123 June 1, 2017.

Alzheimer's and neurodegenerative diseases

An aging population has brought about a global epidemic of unprecedented proportions. Alzheimer's disease (AD) is the most common neurodegenerative disease, and the number of cases reported each year is growing as individual lifespans continue to increase. Worldwide, at least 44 million people are living with dementia, resulting in an annual global cost of approximately $604 billion. By 2030, it is estimated that 76 million people will be living with dementia.

Researchers are attempting to use multiple modalities to diagnose, treat and target the cause of Alzheimer's disease at the molecular level. Anthony Fitzpatrick of the Laboratory of Molecular Biology at the University of Cambridge, UK, recently combined cryo-EM SPA with mass spectrometry to uncover the structure of the tau protein, believed to be a major contributor to Alzheimer's pathology.

Tau filaments are associated with the pathogeny of Alzheimer's disease. They aggregate into macroscopic "tangles" in the brains of Alzheimer's patients. These proteins can be taken directly from patients and then frozen and analyzed with cryo-EM, resulting in a close approximation to in vivo structural conformations.

Other analytical techniques typically focus on fragments of the large tau protein, which provide substantial detail but no context. Cryo-EM, with its ability to image structures close to their native environment, adds this valuable context to the structure determination.

Mass spectrometry improved the determination of sample preparation quality. When combined with cryo-EM, near-atomic resolution structure of the tau protein was determined, revealing potential sites for drug targeting. This groundbreaking work was featured on the cover of Nature in July 2017.

"We used mass spec to validate the structure, the fragments that were constituted, treated with, and broken down. Understanding the phosphorylation sites by mass spec, and also looking at the other proteins that are coming in, what is colocalized in fibers, and what is in tissue…in summary combined proteomics with cryo-EM."

- Anthony W. P. Fitzpatrick, MRC Laboratory of Molecular Biology, Cambridge, UK

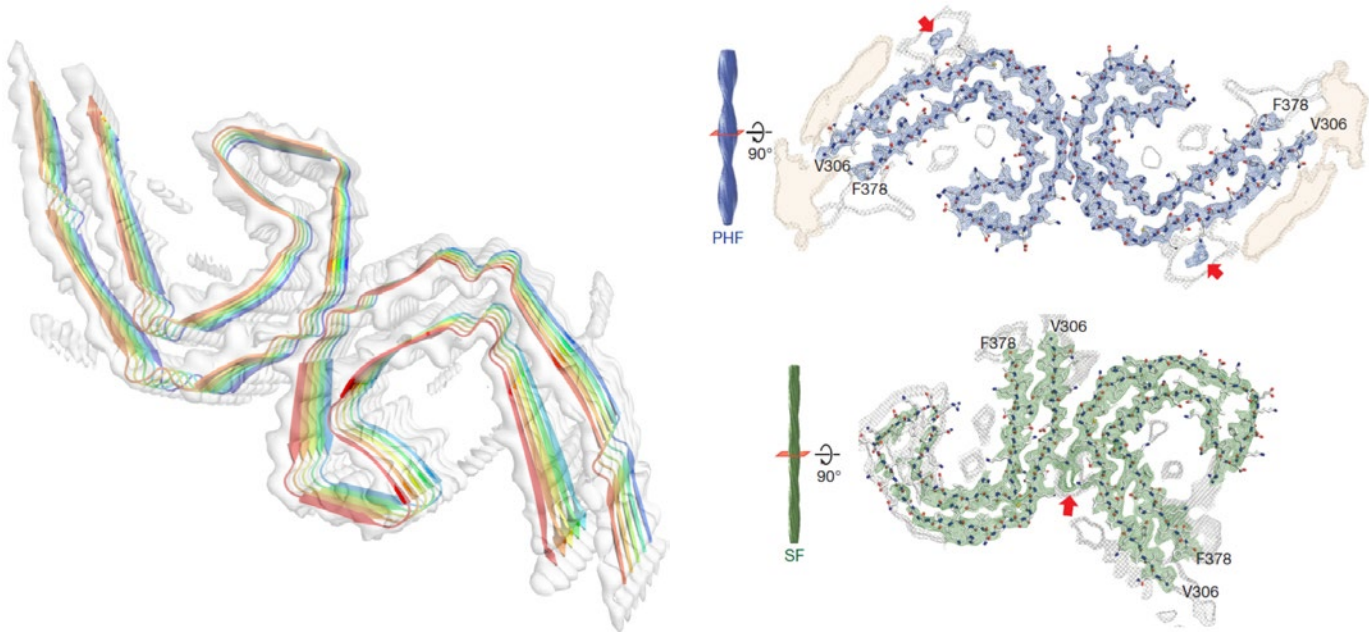

Electron density map (clear) of tau filaments obtained with cryo-EM. The corresponding protein structures (color) neatly fit within the map. Adapted from Fitzpatrick, A.W. et al. Cryo-EM structures of tau filaments from Alzheimer's disease. Nature v. 547, p. 185–190, July 13, 2017.

Atomic details without crystals

Bartesaghi et al. (Structure, v. 26(6), p. 848-856, Jun 5, 2018) were able to clearly visualize the sidechains on a β-galactosidase tetramer by using cryo-EM. Aromatic rings, complete with interior cavities, can even be seen.

Progress in resolution and size

Since 2012, both the minimum size of analytes that can be observed with cryo-EM and the resolution have continuously improved. Now, structures smaller than 0.5 MDa can be visualized at resolutions beyond even 2 Å. While these extremes depend greatly on the symmetry and complexity of the sample, this trend shows the promising trajectory of cryo-EM detail.

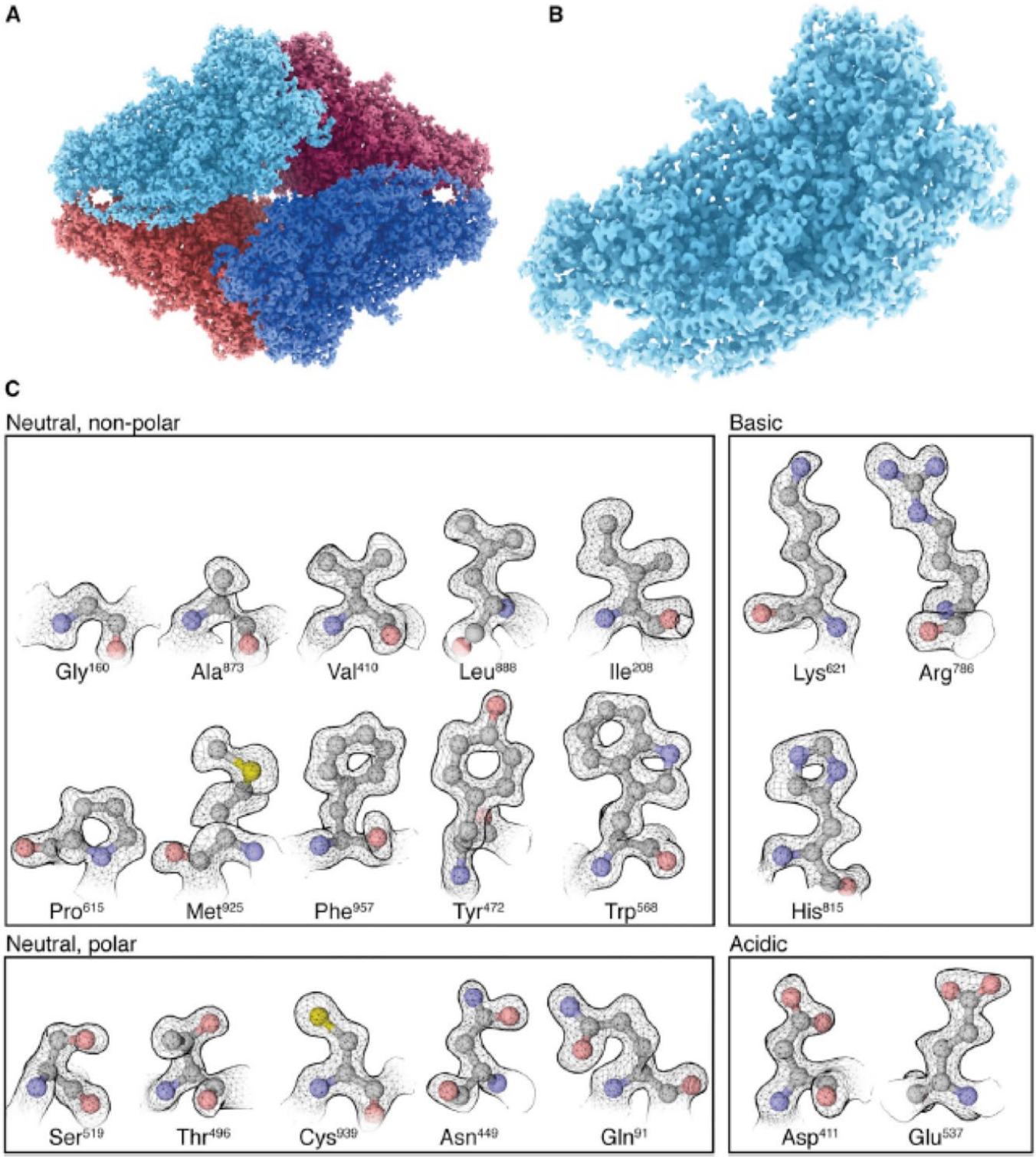

(A) Electron density map of β-galactosidase tetramer determined with cryo-EM. (B) A single β-galactosidase subunit. (C) Electron density maps of individual sidechains corresponding to all 20 major amino acids clearly defined and visualized with cryo-EM. Sidechain conformations determined by molecular dynamics simulations are inset.

"[Recent] advances [in cryo-EM] enable determination of a … density map for β-galactosidase bound to the inhibitor phenylethyl b-D-thiogalactopyranoside where the ordered regions are resolved at a level of detail seen in X-ray maps at ~ 1.5 Å resolution."

- Bartesaghi et al. Structure, v. 26(6), p. 848-856, Jun 5, 2018.

Structures determined with cryo-EM

List reproduced, with permission, from Renaud, J.P. et al. Cryo-EM in drug discovery: achievements, limitations and prospects. Nature Reviews Drug Discovery. v.17, p. 471-492. Jun. 8, 2018. For a complete list, including references, please access the above review.

Object	Reported Resolution
Large and/or dynamic assemblies	
Yeast transcription initiation complex	3.6 Å
Human transcription initiation complex	3.9 Å
Schizosaccharomyces pombe mediator	4.4 Å
Saccharomyces cerevisiae pre-initiation complex	4.7 Å
S. cerevisiae pre-initiation complex—core mediator complex	5.8 Å
Yeast U4/U6.U5 tri-snRNP	3.7 Å
Human U4/U6.U5 tri-snRNP	7 Å
S. pombe spliceosome (mixture of complexes)	3.6 Å
S. cerevisiae pre-catalytic spliceosome (complex B)	3.7 Å
S. cerevisiae activated spliceosome (Bact complex)	3.5 Å
S. cerevisiae activated spliceosome (Bact complex)	5.8 Å
S. cerevisiae spliceosome immediately after branching (complex C)	3.8 Å
S. cerevisiae spliceosome immediately after branching (complex C)	3.4 Å
Human spliceosome just prior to exon ligation (complex C*)	3.8 Å
Human spliceosome just prior to exon ligation (complex C*)	5.9 Å
S. cerevisiae spliceosome just prior to exon ligation (complex C*)	4.0 Å
S. cerevisiae spliceosome just prior to exon ligation (complex C*)	3.8 Å
S. cerevisiae spliceosome immediately after exon ligation (complex P)	3.7 Å
S. cerevisiae spliceosome immediately after exon ligation (complex P)	3.3 Å
Zika virus	3.8 Å
Herpesvirus capsid	3.1 Å
Human actomyosin–tropomyosin complex	3.9 Å
Mouse mammary tumor virus intasome	5 Å
Porcine respiratory supercomplex SCI1III2IV1	4.0 Å
Human respiratory supercomplex SCI1III2IV1	3.9 Å
HIV 1 EnvΔCT in complex with the PGT151 Fab	4.2 Å
Natively glycosylated HIV 1 Env in complex with bnAbs	3.5 Å
Yeast proteasome lid	3.5 Å
Yeast 26S proteasome (two structures)	4.6–4.8 Å
Human 26S proteasome	3.5 Å
Escherichia coli 70S ribosome in complex with SelB and Sec-tRNASec (six intermediate structures)	3.4–5.3 Å
Human 80S ribosome	~3 Å
S. cerevisiae small-subunit processome	3.8 Å
Chaetomium thermophilum 90S pre-ribosome	3.2 Å
S. cerevisiae nucleolar pre 60S ribosomal subunit	3.4 Å
Microtubules in different nucleotide states	3.5 Å
HIV 1 strand transfer complex intasome	~3.5–4.5 Å
197 bp nucleosome in complex with linker histone H1.5DC50	6.2 Å
E. coli relaxase	3.9 Å
Pseudomonas aeruginosa CRISPR RNA-guided surveillance complex bound to AcrF1 and AcrF2	3.4 Å
P. aeruginosa CRISPR RNA-guided surveillance complex bound to target double-stranded DNA	2.9 Å

Object	Reported Resolution
Late-stage assembly intermediates of the human mitoribosomal large subunit	~3 Å
S. cerevisiae cleavage and polyadenylation factor polymerase module	3.5 Å
Human cleavage and polyadenylation specificity factor core module bound to the PAS hexamer motif	3.1 Å
Dynein tail–dynactin–BICDR1 complex	3.5 Å
Polycomb repressive complex 2	4.6 Å
S. cerevisiae oligosaccharyltransferase complex	3.5 Å
GATOR1–RAG GTPase complex	4.0 Å
Activator-bound human translation initiation factor eIF2B	4.1 Å
Activator-bound human translation initiation factor eIF2B	2.8 Å
Insulin receptor extracellular domain–insulin 1:2 complex	4.3 Å
Membrane protein complexes	
Zebrafish α1 glycine receptor in complex with strychnine, glycine and glycine and ivermectin	3.8–3.9 Å
GluK2 in its desensitized state	3.8 Å
Prokaryotic cobalt/magnesium transport protein CorA	3.8 Å
Mammalian voltage-gated calcium channel Cav1.1	3.6 Å
Mammalian voltage-gated potassium channel Kv10.1 (also known as EAG1 or KCNH1)	3.8 Å
Eukaryotic voltage-gated sodium channel NavPaS	3.8 Å
Aplysia californica Ca2+-activated K+ channel	3.5 Å
Caenorhabditis elegans cyclic-nucleotide-gated channel bound to cGMP	3.5 Å
Human hyperpolarization-activated cyclic nucleotide-gated channel in the absence and presence of cAMP	3.5 Å
Serotonin receptor (5 HT3AR)	4.3 Å
Zebrafish cystic fibrosis transmembrane conductance regulator	3.7 Å
Porcine respiratory supercomplex SCI1III2IV1	4.0 Å
Human respiratory supercomplex SCI1III2IV1	3.9 Å
Triheteromeric GluN1–GluN2A–GluN2B glutamate receptor ionotropic, N methyl-d aspartate in complex with a GluN2B specific allosteric modulator	4.5 Å
Bovine MRP1 in presence and absence of leukotriene C4	3.3–3.5 Å
Human calcitonin receptor–salmon calcitonin–G protein heterotrimer	4.1 Å
Rabbit GLP1 receptor–human GLP1–G protein heterotrimer	4.1 Å
Human GLP1 receptor–G protein-biased peptide exendin P5–G protein heterotrimer	3.3 Å
Human adenosine A2A receptor–agonist–engineered G protein heterotrimer	4.5 Å
Voltage-gated potassium channel subunit Kv11.1 (also known as hERG1 or KCNH2)	3.8 Å
Human multidrug transporter ABCG2	3.8 Å
Human multidrug transporter ABCG2 bound to an inhibitor and two Fabs	3.1 Å
Type 1 ryanodine receptor in complex with immunophilin FKBP12 (also known as FKBP1A)	3.8 Å
Type 1 ryanodine receptor in multiple functional states	3.8–4.5 Å
Agonist-bound and antagonist-bound human TRPA1	3.9–4.7 Å
Human TRPML1 channel structures in open and closed conformations	3.5–3.7 Å
Mouse TRPML1 channel embedded in nanodiscs	3.6 Å
Common marmoset TRPML3 channel	2.9 Å
Human TRPM4 bound to Ca2+ and a modulator	3.8 Å
Mouse TRPM4 in the ATP-bound and apo states	2.9–3.1 Å
Mammalian SUR1–inward rectifier K+ channel Kir6.2 channel bound to glibenclamide and ATP	3.6 Å
Unliganded, agonist-bound and antagonist-bound rat TRPV1	2.9–3.4 Å

thermo scientific

Object	Reported Resolution
Rabbit TRPV2	~4 Å
Xenopus tropicalis TRPV4	3.8 Å
Rabbit TRPV5 in the presence of econazole	4.8 Å
Human PC2 (also known as PKD2) channel in lipid nanodiscs	3.0 Å
Nanodisc-reconstituted yeast vacuolar ATPase Vo proton channel	3.5 Å
Mammalian voltage-dependent calcium channel TPC1 in the presence and absence of phos¬phatidylinositol 3,5 bisphosphate	3.2–3.4 Å
Blastochloris viridis light-harvesting 1–reaction centre (LH1–RC) complex	2.9 Å
Flavobacterium johnsoniae alternative complex III alone and in supercomplex with cytochrome c oxidase aa3	3.6 Å
27 fold and 28 fold single-ring pores formed by the amino terminal fragment of mouse gasdermin A3	3.8–4.2 Å
Ever-smaller objects	
Human peroxiredoxin 3 dodecamer (257 kDa)	4.4 Å
Nucleosome core particle (200 kDa)	3.9 Å
Human γ secretase (~170 kDa + 30–70 kDa from glycosylation)	3.4 Å
Human peptide transporter TAP in complex with the herpesvirus ICP47 protein (166 kDa)	6.5 Å
Human calcitonin receptor–salmon calcitonin–G protein heterotrimer (~150 kDa)	4.1 Å
Chicken heart lactate dehydrogenase B in complex with an inhibitor (145 kDa)	2.8 Å
Human isocitrate dehydrogenase 1 R132C in the absence and presence of an inhibitor (93 kDa)	3.8 Å
Human haemoglobin (64 kDa)	3.2 Å
Objects at high resolution, including complexes with small molecules	
E. coli 70S ribosome in complex with elongation factor Tu and kirromycina	2.9 Å
P. aeruginosa CRISPR RNA-guided surveillance complex bound to target double-stranded DNA	2.9 Å
Common marmoset TRPML3 channel	2.9 Å
ATP-bound mouse TRPM4b	2.9 Å
Agonist-bound rat TRPV1b	2.9 Å
B. viridis light-harvesting 1–reaction centre (LH1–RC) complex	2.9 Å
Adeno-associated virus AAV DJ (gene therapy vector) in complex with fondaparinux	2.8 Å
Thermoplasma acidophilum 20S proteasome	2.8 Å
Chicken heart lactate dehydrogenase B in complex with an inhibitor	2.8 Å
Rabbit muscle aldolasec	2.6 Å
Leishmania donovani ribosome in complex with paromomycin	2.5–2.7 Å
Trypanosoma cruzi ribosome large subunit	2.5 Å
T. acidophilum 20S proteasomed	2.4 Å
Human AAA+ ATPase p97 in presence and absence of an allosteric inhibitor	2.3–2.4 Å
Rhinovirus B14 in complex with the C5 Fab	2.3 Å
β Galactosidase in complex with a cell-permeant inhibitor	2.2 Å
Bovine glutamate dehydrogenasee	1.8 Å

Find out more at **pharmadrugdiscovery.com**

ThermoFisher SCIENTIFIC